DIELECTRIC SPECTROSCOPY MAPPING OF SUBSURFACE ICE ON THE MOON AND MARS. D. E. Stillman and R. E. Grimm, Department of Space Studies, Southwest Research Institute, 1050 Walnut Street, Suite 400, Boulder, CO 80302, dstillman@boulder.swri.edu, grimm@boulder.swri.edu.

Introduction: Subsurface water ice is thought to exist in shallow-subsurface cold traps near the poles of the Moon and at high latitudes on Mars [1,2,3]. Neutron spectroscopy has provided these important insights, yet is limited in depth of investigation to several tens of centimeters and cannot uniquely identify water ice as the host of the detected element, hydrogen. Measurement of electrical properties can, however, uniquely identify water ice from its low-frequency dielectric relaxation. Furthermore, ice concentration can be estimated as a function of depth by changing the electrode geometry. Laboratory measurements of pure ice, doped ice, and regolith-ice mixtures will better characterize the magnitude of the ice response and its mechanism, and new instrument designs will optimize the method for lunar and martian applications in the next decade.

Dielectric Relaxation of Ice: Dispersion in the dielectric constant arises from frequency dependence in polarizability and is often manifested as a distinct band of maximum change, a dielectric relaxation (Fig. 1). Bjerrum defects in water ice are strongly polarized at low frequencies to create a real part of the relative dielectric permittivity at low frequency (ε'_{DC}) >80 [4]. At high frequency, these defects cannot move fast enough to polarize fully, limiting the real part of the relative dielectric permittivity there to ~3. The Debye relaxation frequency occurs at the frequency where these defects are in constant motion.

The relaxation frequency and ε'_{DC} are dependent on temperature, the amount of excess H^+ and OH^-, and the amount of Cl^- and F^- impurities that have replaced O^{2-} in the lattice structure of ice [4]. The temperature dependence of the relaxation frequency follows an Arrehenius relationship with an activation energy of ≈0.56 eV at >233 K (this temperature increases as the amount of impurities in the ice lattice increase) and an activation energy of ≈0.23 eV at low temperatures [4]. The value of activation energy describes how quickly relaxation frequency changes with temperature. At warmer temperatures, the Bjerrum defects are able to migrate faster because they possess more thermal energy. Decreasing temperature increases ε'_{DC} by reducing the thermal energy of the defects and allowing them to stay better aligned with the electric field. Cl^- and F^- impurities create more Bjerrum defects and allow them to migrate faster, thus increasing both ε'_{DC} and the relaxation frequency [4]. Likewise, H^+ and OH^- impurities also increase both the ε'_{DC} and the relaxation frequency [4].

Laboratory Measurement: The dielectric relaxation of pure and doped ice has been measured previously; however much uncertainty remains in these measurements at temperatures below 233 K [4,5]. Little research has been conducted on the effects of ice in soil [6,7]. Extrapolations from existing data show that the ice relaxation at the temperature of the permanently shadowed lunar craters (≈100 K) is most likely greater than 10^{-5} Hz (Fig 2). To reduce this uncertainty, temperature and frequency dependent electrical property measurements of soil/ice mixtures as well as pure and doped ice samples have and are currently being measured over a temperature range from 90 – 273 K and frequency range from 1 mHz – 1 MHz. Electrical properties measurements are being made with a 1260 Solartron Impedance Analyzer connected to a 1296 Dielectric Interface or a 1294 Impedance Interface. Measurements can be made in both three-electrode and four-electrode geometries [8]. Electrical properties can be expressed as complex dielectric constant, complex conductivity, or complex resistivity.

Application: Narrowband measurement of the resistive-capacitive properties of the earth ("induced polarization") has been used for nearly a century to explore for minerals and groundwater and to characterize subsurface geology. Broadband systems are now seeing wide application, including environmental studies [e.g., 9]. The Huygens, the Rosetta lander, and Phoenix spacecraft all include electrical-properties sensors. However, characterization of the full bandwidth of possible water-ice responses and soundings to depths of meters or more requires high-impedance (~10 TΩ), low-capacitance (~1 pF) coupling, mitigation of coherent noise such as leakage and eddy currents using buffering shielding, guarding of electrodes, and larger electrode arrays. The electrodes (sensors) can be accommodated in lander legs, rover wheels, a robotic arm, or in a ballistically deployed string (Fig. 3). Our present efforts are aimed toward a design of transmitter and receiver requiring a few kilograms and a few watts, plus sensors.

A forward calculation using present estimates of the intrinsic properties of ice and its moderation due to regolith mixing (Fig. 4) illustrates that an ice-detection limit of ~1% or better is possible.

References: [1] Vasavada, A.R. et al. (1999) *Icarus, 141*, 179-193. [2] Feldman, W.C. et al. (2001) *JGR, 106,* 23231-23252. [3] Feldman, W.C. (2002) *Science, 197*, 75-78 [4] Petrenko V.F. and Whitworth R.W. (1999) *Physics of Ice*, 373 pp. [5] Johari G.P. and Whalley E. (1981) *J. Chem. Phys., 75*, 1333-1340. [6] Alvarez R. (1973) *Earth & Planet. Sci. Let., 20*, 409-414. [7] Alvarez R. (1973) *Science, 179*, 1122-1123. [8] Olhoeft, G.R. (1985), *Geophys.*, 50, 2492-2503. [9] Grimm R.E. (2005) *J. Environ. Eng. Geophys., 10*, 351-364. [10] Auty, R.P. and Cole R.J. (1952) *J. Chem. Phys., 20*, 1309. [11] Kawada, S. (1978) *J. Phys. Soc. Jpn.*, 44, 1881-1886. [12] Johari, G.P. and Jones J. (1975) *J. Chem. Phys.*, 62, 4213. [13] Telford W.M. et al. (1990) *Applied Geophysics*, 770 pp. [14] Carrier, W.D. (1991) in *Lunar Sourcebook (eds. Heiken et al.)*, 475-594.

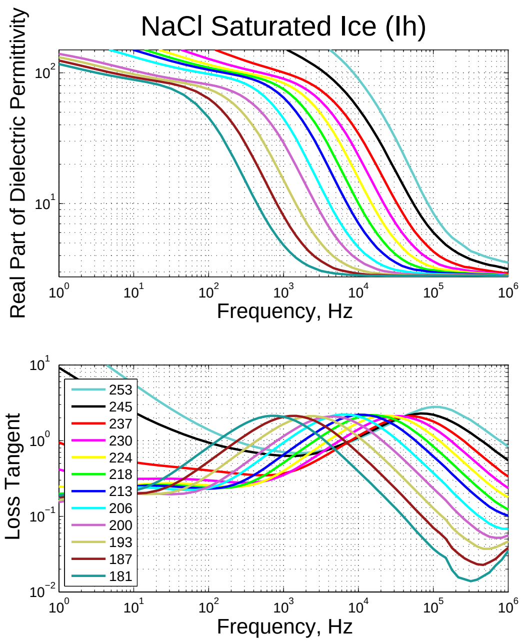

Fig. 1. Temperature and frequency dependence of NaCl saturated ice (Ih). Low frequency limit of the real part of the dielectric permittivity is never attained due to electrode polarization.

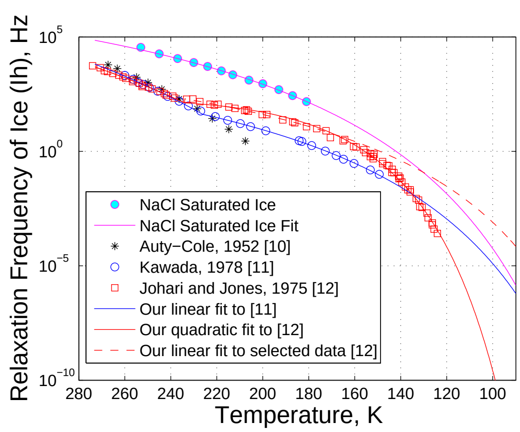

Fig. 2. Data and models of the dielectric relaxation frequency of ice (Ih) versus temperature. Pure ice is shown in the previous measurements [10,11,12]. Note that as Cl^- impurities replace O^{2-} the relaxation frequency is greatly increased.

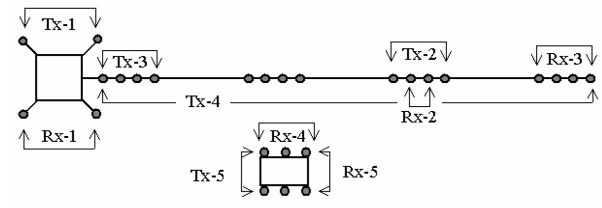

Figure 3. Alternative schematic layouts for IP electrodes. Tx = transmitter, Rx = receiver. (1) Electrodes on static lander footpads. (2) Closely spaced electrodes on ballistically deployed string for shallow subsurface investigation. (3) Widely spaced electrodes for deeper investigation. (4) Large transmitter dipole on lander and short dipole on rover (wheel base) for deep investigation. (5) Rover-only short dipoles for mobile, shallow investigation.

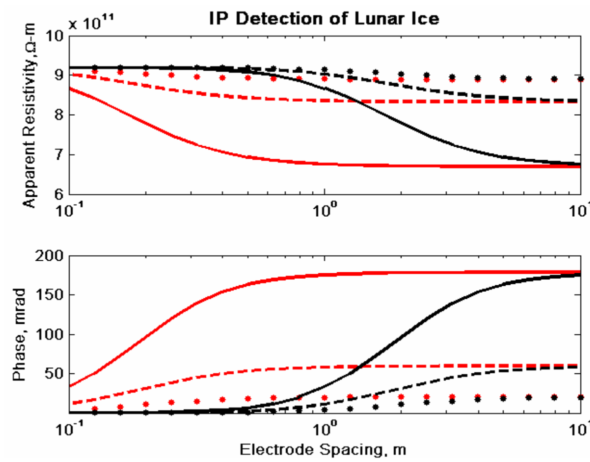

Fig. 4. Forward models for the geoelectrical signature of lunar ice from surface electrode arrays. Model invokes a two-layered structure [13], uses the complex refractive index model (CRIM) to calculate electrical properties of mixtures of soil and the target substance, and assumes that multiple electrodes are distributed along a linear antenna such that four-electrode combinations can be used at a variety of spatial scales. Ice depths of 0.1 m (red) and 1 m (black) and ice fractions 10% (solid), 3% (dash), and 1% (dot) indicate that ice can be resolved at percent abundance or better (relaxation time constant of ice after Kawada [11]; dry regolith resistivity 10^{12} Ω-m after Carrier et al. [14]; test frequency 1 mHz).